P273

# Anti-aliasing Filter for Reverse-time Migration

G. Zhan* (KAUST) & G.T. Schuster (KAUST)

## SUMMARY

We develop an anti-aliasing filter for reverse-time migration (RTM). It is similar to the traditional anti-aliasing filter used for Kirchhoff migration in that it low-pass filters the migration operator so that the dominant wavelength in the operator is greater than two times the trace sampling interval, except it is applied to both primary and multiple reflection events. Instead of applying this filter to the data in the traditional RTM operation, we apply the anti-aliasing filter to the generalized diffraction-stack migration operator. This gives the same migration image as computed by anti-aliased RTM.

## Introduction and Method

A prestack migration image $m(\mathbf{x})$ for a common shot gather (CSG) can be computed with the diffraction-stack migration formula:

$$m(\mathbf{x}) \quad = \quad \sum_{\omega}\sum_{g} \alpha(\omega,\mathbf{x},\mathbf{g},\mathbf{s}) \overbrace{[G(\mathbf{g}|\mathbf{x})^* G(\mathbf{x}|\mathbf{s})^*]}^{migration\ kernel} \overbrace{D(\mathbf{g}|\mathbf{s})}^{CSG}, \tag{1}$$

where $D(\mathbf{g}|\mathbf{s})$ is the CSG in the frequency domain for a shot at $\mathbf{s}$ and geophone at $\mathbf{g}$, $G(\mathbf{x}|\mathbf{s})$ is the background Green's function which is a solution to the acoustic Helmholtz equation for a source at $\mathbf{s}$ and observed at $\mathbf{x}$, and $m(\mathbf{x})$ is the migration image at the trial image point $\mathbf{x}$. Here, the $G(\mathbf{x}|\mathbf{x}')$ ($\mathbf{x}'$ may be at $\mathbf{x}$ or $\mathbf{g}$) and $D(\mathbf{g}|\mathbf{s})$ spectra depend on angular frequency $\omega$, but its notation is silent. The preconditioning function $\alpha(\omega,\mathbf{x},\mathbf{g},\mathbf{s})$ is defined by the user, and can compensate for the band-limited source wavelet, obliquity factor, acquisition footprint, and geometrical spreading.

If $G(\mathbf{x}|\mathbf{x}')$ is the asymptotic Green's function computed by ray tracing and only accounts for single scattering events, then equation 1 is the general formula for Kirchhoff migration (KM). The KM point scatterer response of $\sum_{\omega}\sum_{g}\alpha(\omega,\mathbf{x},\mathbf{g},\mathbf{s})\ G(\mathbf{g}|\mathbf{x})^* G(\mathbf{x}|\mathbf{s})^* D(\mathbf{g}|\mathbf{s})$ is computed by specifying a trial image point at $\mathbf{x}$ and summing the energy in the CSG along the hyperbola-like colored curves in Figure 1a. This summed energy value is placed at $\mathbf{x}$ and the result is the migration image $m(\mathbf{x})$, and only accounts for primary reflections in the data.

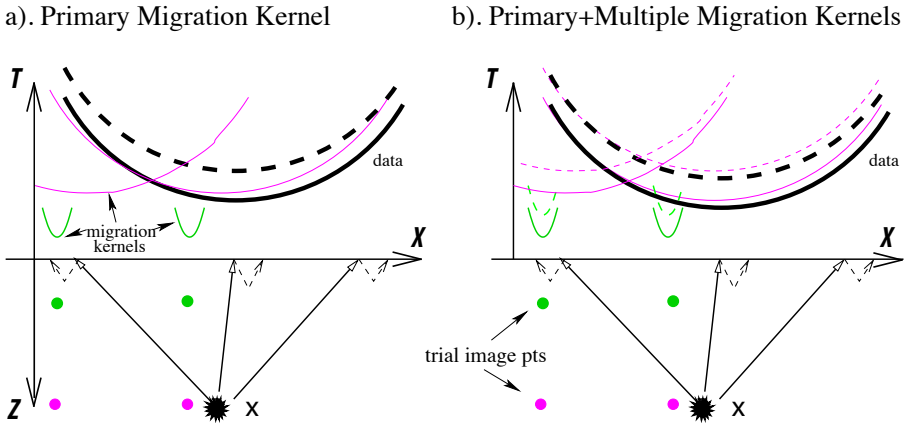


***Figure 1*** *Migration kernels plotted in data space as colored hyperbolas for a) primary and b) primary+multiple events associated with shallow (green) and deep (pink) trial image points. The best match between the data (black hyperbolas) and migration curves (pink and green) is when the trial image point is near the actual scatterer's position; the dot-product between the migration kernel and data fingerprints will give the greatest value when the trial image point is at the actual scatterer's location.*

*Migration as Fingerprint Matching.*

This migration operation can also be interpreted as a dot-product of the kernel fingerprint $G(\mathbf{g}|\mathbf{x})G(\mathbf{x}|\mathbf{s})$ with the CSG fingerprint $D(\mathbf{g}|\mathbf{s})$ (Schuster, 2002), and the result is $m(\mathbf{x})$. If the trial image point is at an actual scatterer, then the fingerprints of the CSG and migration kernel will be a good match and the dot-product will return a large value. If the trial image point is far from any reflector, then the CSG and kernel fingerprints will be mismatched and the dot-product will yield a low magnitude. This description defines the dot-product interpretation of migration, and we will now refer to $G(\mathbf{g}|\mathbf{x})G(\mathbf{x}|\mathbf{s})$ and $D(\mathbf{g}|\mathbf{s})$ as kernel and data fingerprints, respectively.

*Anti-aliasing Filter for KM.*

The anti-aliasing condition for the KM operator (Gray, 1992; Lumley et al., 1994; Abma et al., 1999; Biondi, 2001; Zhang et al., 2003) says that the local slope $dt/dx$ (e.g., computed from the traveltime table) of the associated hyperbola diffraction curve in $x-t$ space should satisfy the Nyquist sampling criterion:

$$\left|\frac{dt}{dx}\right| \leq \frac{T}{2\Delta x} = \frac{1}{2f\Delta x}, \tag{2}$$

where $T$ is the minimum period in the data at frequency $f$, and $\Delta x$ is the input trace spacing. If this condition is not satisfied for any $(x,t)$ sample in the CSG, the local portion of this trace at time $t$ is high-cut filtered to $f_{cut} = 1/(2\Delta x)/|dt/dx|$ to eliminate the offending high-frequency components.

*Anti-aliasing Filter for RTM.*

If $G(\mathbf{x}|\mathbf{x}')$ is computed by a finite-difference solution to the wave equation, then equation 1 defines the RTM formula. Its traditional implementation (Stolt and Benson, 1986) is to backpropagate the data and take the zero-lag correlation of it with the forward propagated field to get $m(\mathbf{x})$. An alternative implementation+interpretation of RTM is provided by generalized diffraction-stack migration (GDM). Schuster (2002) showed that the RTM image at $\mathbf{x}$ can be implemented as a dot-product of the kernel fingerprint $\mathscr{F}^{-1}[G(\mathbf{g}|\mathbf{x})G(\mathbf{x}|\mathbf{s})]$ with that of the CSG fingerprint $\mathscr{F}^{-1}[D(\mathbf{g}|\mathbf{s})]$, where $\mathscr{F}^{-1}[\,]$ represents the inverse Fourier transform. In either the RTM or GDM implementations, the resulting migration images are identical.

As an example, Figure 1b shows that the kernel fingerprint consists of several hyperbolas for a specified image point $\mathbf{x}$. The early arriving hyperbola is for the primary scattering and the later one is associated with a multiple. Therefore, the anti-aliasing strategy for RTM consists of the following:

1. Define $g(\mathbf{g},t|\mathbf{x}) = \mathscr{F}^{-1}[G(\mathbf{g}|\mathbf{x})]$. Use a finite-difference solution to the space-time wave equation to compute $g(\mathbf{g},t|\mathbf{x})$ for a source at $\mathbf{x}$ and geophone at $\mathbf{g}$. Here $\mathbf{x}$ is in the model space.
2. Convolve $g(\mathbf{g},t|\mathbf{x})$ with $g(\mathbf{s},t|\mathbf{x})$ to get the kernel fingerprint (RTM migration kernel) $g(\mathbf{x},\mathbf{s},\mathbf{g},t) = g(\mathbf{g},t|\mathbf{x}) * g(\mathbf{x},t|\mathbf{s})$, where $*$ denotes temporal convolution. The convolution results are the colored-line hyperbolas shown in Figure 1b.
3. Apply local low-pass filters to every time sample of this kernel so that the anti-aliasing condition 2 is satisfied. Denote this filtered kernel fingerprint as $\tilde{g}(\mathbf{x},\mathbf{s},\mathbf{g},t)$.
4. Take dot-products of $\tilde{g}(\mathbf{x},\mathbf{s},\mathbf{g},t)$ with $d(\mathbf{g},t|\mathbf{s})$ to get the prestack migration image $m(\mathbf{x})$ for a single shot at $\mathbf{s}$. The resulting image will be free of aliasing artifacts.

**Results**

Synthetic tests associated with a fan model (Figure 2a) are presented to demonstrate the effectiveness of the proposed RTM anti-aliasing filter. The velocity model shown in Figure 2a has a homogeneous background velocity of 2000 $m/s$ perturbed by a series of dipping events and deep scatterers with a higher velocity of 2500 $m/s$. Figure 2b displays a typical CSG for this model calculated by a finite-difference (FD) solution to the two-way wave equation. Fifty-one CSGs are computed with the shot interval of 160 $m$, and the first shot is fired at $X = 2$ $km$. A fixed spread is used and 301 traces are recorded along the surface with a trace interval of 40 $m$. The peak frequency of the Ricker wavelet is 15 $Hz$ and the record length is 6 $s$. Both reflections and diffractions can be clearly seen in the CSG.

Before doing RTM, we first apply the Kirchhoff migration (KM) to this synthetic data set to illustrate the migration aliasing problem for this model. Figure 3a shows a CSG with the surface shot at $sx = 7.6$ $km$,

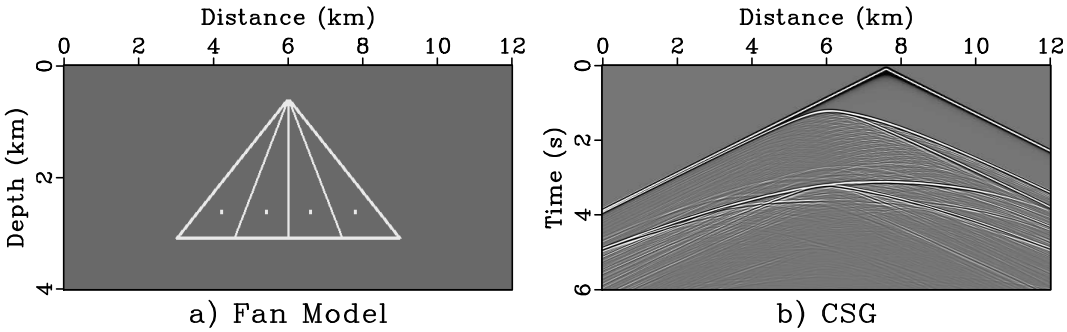


***Figure 2*** *a) Synthetic velocity model used in the anti-aliasing tests. The background velocity (gray color) is* 2000 $m/s$ *and the perturbed velocity (white color) is* 2500 $m/s$. *b) A typical shot gather at* $X = 7.6$ *km.*

where the direct waves are removed. Figure 3b depicts the KM operator, which is a hyperbola for a fixed trial image point at $\mathbf{x}$ (located at $X = 6$ *km* and $Z = 3$ *km*). The KM operation for a trial image point $\mathbf{x}$ can be viewed as summing energy along this hyperbola. Figures 3c and 3d are the corresponding stacked KM images for 51 CSGs with and without applying an anti-aliasing filter. Aliasing artifacts are visible in Figure 3c and are then suppressed with a KM anti-aliasing filter proposed by Lumley et al. (1994).

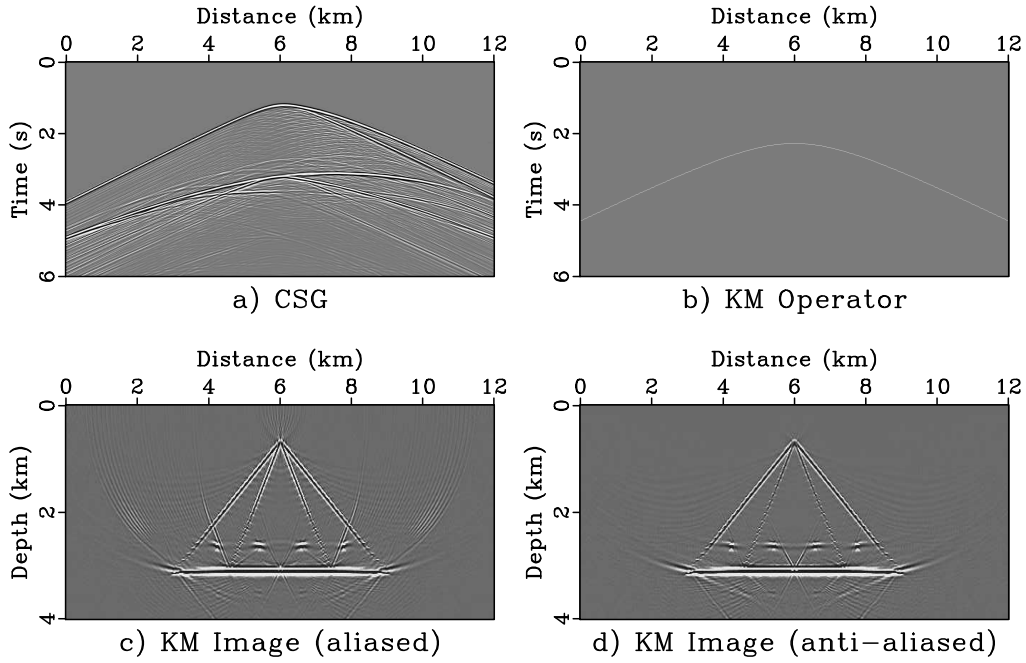


***Figure 3*** *Kirchhoff migration (KM) examples.*

The RTM anti-aliasing filter described in the theory part is now applied to the same synthetic data. Figure 4b presents the RTM operator for the same trial image point and CSG shown in Figure 3b. Unlike the hyperbola traveltime curve for the KM operator, the RTM operator contains both primary and multiples along with amplitude and phase information. Figure 4c shows the stacked RTM image of this model. Aliasing artifacts seen in the standard RTM image are similar to those in Figure 3c. The RTM anti-aliasing filter is then constructed using the proposed approach and applied to the RTM operator to eliminate the offending high-frequency components. Figure 4d displays the RTM image with the anti-aliasing filtering applied. Compared to Figure 4c, the aliasing artifacts are largely eliminated with the usage of this filter.

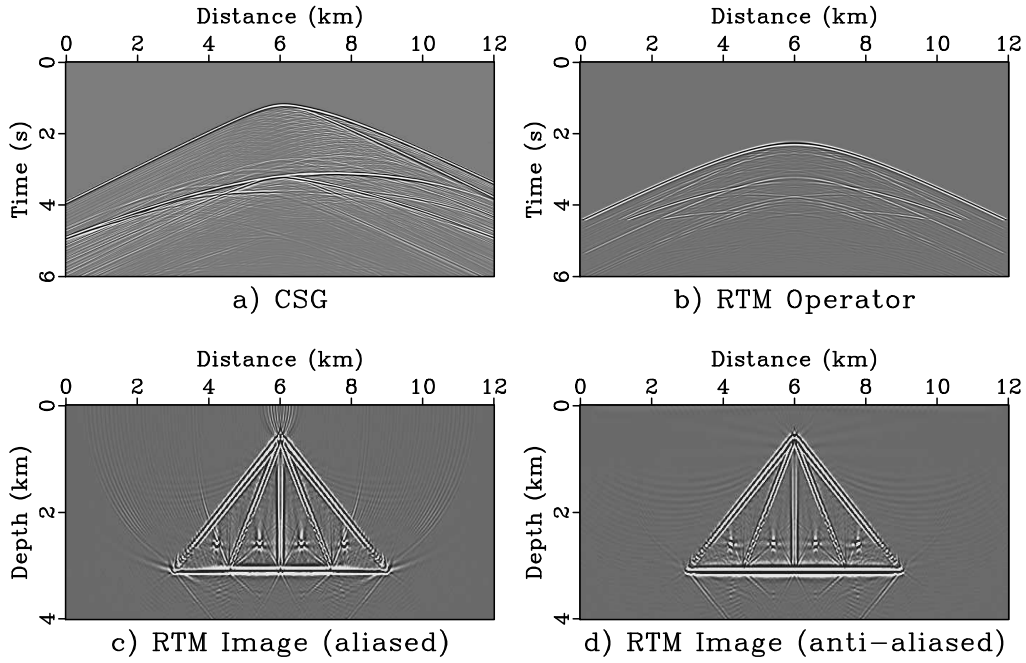


***Figure 4*** *Reverse-time migration (RTM) examples.*

## Summary and Discussion

We proposed an anti-aliasing filter for reverse time migration (RTM). It is similar to the traditional anti-aliasing filter used for Kirchhoff except that it now accounts for both primary and multiple reflection events. The anti-aliasing filter is applied to the generalized diffraction-stack migration operator, which gives the same migration image as computed by an anti-aliased RTM. Numerical results verified the effectiveness of this procedure. The main disadvantage of applying this anti-aliasing filter is the increased computational cost compared to standard RTM, except in a target-oriented mode. An alternative to anti-aliased RTM is least squares migration (LSM) or migration deconvolution (MD). It is observed that LSM (Nemeth et al., 1997) and MD (Yu et al., 2006) appear to overcome aliasing problems and, unlike the traditional anti-aliasing filter, does not low-pass filter the data. Until recently, LSM was computationally expensive, but Dai et al. (2011) shows that a phase encoded multisource formulation makes it no more expensive than standard RTM. Therefore, MD and LSM might be a viable alternative to an explicit low-pass anti-aliasing filter applied to the data.

## References

Abma, R., Sun, J. and Bernitsas, N. [1999] Anti-aliasing methods in Kirchhoff migration. *Geophysics*, **64**, 1783–1792.

Biondi, B. [2001] Kirchhoff imaging beyond aliasing. *Geophysics*, **66**, 654–666.

Dai, W., Schuster, G.T., and Fowler, P. [2011] Multisource least squares reverse time migration. *Geophysical Prospecting (in press)*.

Gray, S.H. [1992] Frequency-selective design of the Kirchhoff migration operator. *Geophysical Prospecting*, **40**, 565-571.

Lumley, D. E., Claerbout, J.F. and Bevc D.[1994] Anti-aliased Kirchhoff 3-D migration. *SEG Expanded Abstracts*, **13**, 1282–1285.

Nemeth, T., Wu, C., Schuster, G.T. [1999] Least-squares migration of incomplete reflection data. *Geophysics*, **64**, 208–221.

Schuster, G.T. [2002] Reverse-time migration = generalized diffraction stack migration. *SEG Expanded Abstracts*, **21**, 1280–1283.

Stolt, R. and Benson, A. [1986] Seismic migration: theory and practice, in *Handbook of Geophysical Exploration*, Volume **5**, *Geophysical Press*, London, UK.

Yu, J., Hu, J., Schuster, G.T. and Estill, R. [2006] Prestack migration deconvolution. *Geophysics*, **71**, S53–S62.

Zhang, Y., Sun, J. and Gray, S. [2003] Aliasing in wavefield extrapolation prestack migration. *Geophysics*, **68**, 629–633.